Proceedings of the International Conference on Oxide Materials for Electronic Engineering, May 29–June 2, 2017, Lviv

Photoluminescence and Thermoluminescence of the Oxygen-Deficient YAG, YAP, and YAM Phosphors

Ya. Zhydachevskyy[a,b,*], I. Kamińska[a], M. Glowacki[a], A. Kilian[c], S. Ubizskii[b], P. Bilski[c], M. Berkowski[a], K. Fronc[a], D. Elbaum[a] and A. Suchocki[a,d]

[a]Institute of Physics, Polish Academy of Sciences, Al. Lotnikow 32/46, PL-02668 Warsaw, Poland

[b]Lviv Polytechnic National University, S. Bandera 12, Lviv 79646, Ukraine

[c]Institute of Nuclear Physics, Polish Academy of Sciences, E. Radzikowskiego 152, 31-342 Krakow, Poland

[d]Institute of Physics, University of Bydgoszcz, J. Weyssenhoffa 11, 85-072 Bydgoszcz, Poland

Photoluminescence and thermoluminescence of the oxygen-deficient $Y_3Al_5O_{12}$ (YAG), $YAlO_3$ (YAP) and $Y_4Al_2O_9$ (YAM) ceramics has been studied. Corresponding ceramic samples prepared by the same way however in oxidizing conditions (in air) were studied for comparison. The observed luminescent properties of the materials are related to the F-type centers created on the basis of oxygen vacancies, antisite (Y_{Al}) defects and uncontrolled Tb^{3+} impurity ions.

DOI: 10.12693/APhysPolA.133.977

PACS/topics: 78.55.Hx

1. Introduction

Application potential of the carbon-doped $Y_3Al_5O_{12}$ (YAG:C) for radiation dosimetry using the thermoluminescence (TL) or the optically stimulated luminescence (OSL) techniques has been shown recently [1]. In particular, the OSL sensitivity of the non-optimized YAG:C to β-radiation (^{90}Sr/^{90}Y, 10 mGy) was found to be about 0.1 of the commercial α-Al_2O_3:C (Landauer Inc., USA). The oxygen-deficient aluminum oxide (Al_2O_3:C) is well-known TL and OSL phosphor that exploits luminescence of F centers created on the basis of oxygen vacancies in the material (see e.g. [2–4]). Therefore it is of interest to evaluate features of other oxygen-deficient oxide compounds.

The present study is aimed to check the photoluminescent and thermoluminescent properties of the oxygen-deficient YAG phosphor and to compare them with other yttrium-aluminum oxides of YAP and YAM obtained in similar oxygen-deficient conditions. The paper presents results on photoluminescence (PL), photoluminescence excitation (PLE) and TL measurements of the phosphors after exposure to UV light (250–350 nm) or ionizing γ-(^{60}Co) and β-(^{90}Sr/^{90}Y) radiations.

2. Materials and methods

The nominally pure compounds of $Y_3Al_5O_{12}$, $YAlO_3$ and $Y_4Al_2O_9$ in the form of nanopowders were synthesized by the solution combustion method using urea as a fuel similarly as described in [5]. The solid ceramic samples were prepared from the obtained nanopowders by pressing of pellets (12 mm in diameter and 3 mm thickness) and after that annealing at 1000–1500 °C in strongly reducing conditions (pure N_2 gas atmosphere + graphite equipment). Besides, additional doping with carbon by means of mixing of the starting powders with graphite powder (from 1 to 5 wt%) was used. Ceramic samples prepared from the same nanopowders however annealed in oxidizing conditions (in air) without any carbon doping were studied for comparison as well. For photoluminescence and thermoluminescence studies, ceramic samples were cut from the pellets into chips of dimensions $3 \times 3 \times 1$ mm^3. The list of studied materials is presented in Table I.

Phase composition and crystallinity of the studied powder and ceramic materials were controlled by the X-ray powder diffraction (XRD) and scanning electron microscopy (SEM) techniques.

The PL and PLE spectra were measured using a Horiba/Jobin-Yvon Fluorolog-3 spectrofluorimeter with a 450 W continuous xenon lamp and a Hamamatsu R928P photomultiplier. The measured PLE spectra were corrected by the xenon lamp emission spectrum.

Irradiation of the samples with γ-rays was performed at room temperature using a ^{60}Co source with the dose rate about 0.6 kGy/h. Typically the studied detectors were stored and irradiated in darkness (wrapped in thin aluminum foil). Before each irradiation procedure the samples were annealed at 500 °C at least for 5 min to erase any possible TL signal due to previous irradiations.

TL readout of the studied samples was performed using a RisøTL/OSL Reader Model DA-20 with a bialkali EMI 9235QB photomultiplier. The β- irradiation source (^{90}Sr/^{90}Y) of the reader was also used for irradiation of the studied samples.

*corresponding author; e-mail: zhydach@ifpan.edu.pl

TABLE I

The list of studied materials

Material and sample notation		Preparation peculiarities	XRD
$Y_3Al_5O_{12}$	YAG powder	powder as synthesized	crystalline, pure YAG phase
	YAG	ceramics from powder as synthesized (1500 °C, 6 h, air)	— // —
	YAG:C	ceramics from powder as synthesized (1500 °C, 6 h, N_2 gas), graphite equipment	— // —
	YAG:C(2%)	— // — &carbon doping (2 wt% of graphite)	— // —
	YAG:C(5%)	— // — &carbon doping (5 wt% of graphite)	— // —
$YAlO_3$	YAP powder	powder as synthesized	crystalline, main YAP phase
	YAP	ceramics from powder as synthesized (1200 °C, 6 h, air)	— // —
	YAP:C	ceramics from powder as synthesized (1200 °C, 2 h, N_2 gas), graphite equipment	— // —
	YAP:C(5%)	— // — &carbon doping (5 wt% of graphite)	— // —
$Y_4Al_2O_9$	YAM powder	powder as synthesized	amorphous, partly crystalline
	YAM powder	powder calcinated in air (1000 °C, 2 h)	crystalline, main YAM phase
	YAM	ceramics from powder calcinated in air (1000 °C, 2 h, air)	— // —
	YAM:C	ceramics from powder calcinated in air (1000 °C, 2 h, N_2 gas), graphite equipment	— // —
	YAM:C(5%)	— // — &carbon doping (5 wt% of graphite)	— // —

3. Results and discussion

Typical X-ray diffraction patterns of the studied powder samples are shown in Fig. 1. These results testify crystalline structure of YAG and YAP powder as synthesized, whereas the YAM powder as synthesized was revealed to be amorphous. Only after next calcination at 1000 °C, the YAM powder becomes crystalline with main $Y_4Al_2O_9$ phase composition (see Fig. 1d). X-ray diffraction patterns of the ceramic samples correspond to the patterns of the powders the ceramic samples were prepared from.

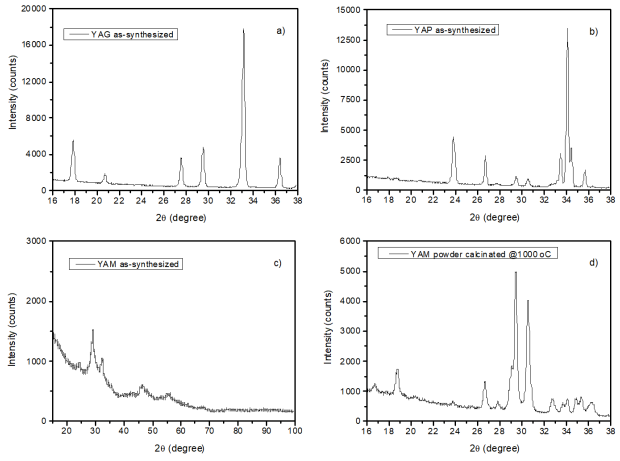

Fig. 1. X-ray diffraction patterns of the studied powder samples.

PL spectra of the studied YAG and YAG:C ceramic samples at UV excitation are shown in Fig. 2. Both YAG and oxygen-deficient YAG (YAG:C) samples demonstrates a characteristic emission with number of narrow lines with major ones at 384, 418, 438, 488 and 544 nm. This emission is excited in single broad band at 273 nm (see Fig. 3) and is caused evidently by Tb^{3+} ions present in the studied material as an uncontrolled impurity satellite to yttrium. It should be mentioned that the same emission of Tb^{3+} was observed in TL emission of YAG:C studied in [1].

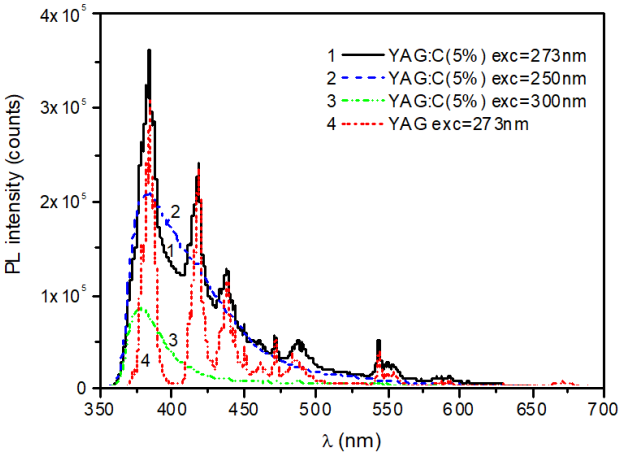

Fig. 2. Room temperature PL spectra of YAG (a) and YAG:C (b) ceramic samples at different wavelength of UV excitation.

Beside the Tb^{3+} emission, the oxygen-deficient YAG samples demonstrate a broad emission band peaked at 380 nm and having a long-wave tail stretching up to 650 nm, that is excited mainly in the band at 250 nm and minor bands at 290 and 305 nm. It is noteworthy that the excitation band at 250 nm is observed only for the oxygen-deficient YAG samples and its relative intensity increases with increase of carbon content. In such a way we believe that the broad emission at 380 nm that

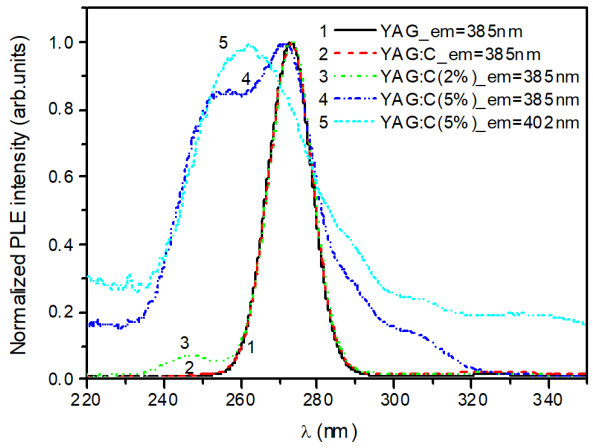

Fig. 3. Room temperature PLE spectra of YAG and YAG:C ceramic samples registered for different emission wavelengths.

is excited at 250 nm is related to F-type centers created on the basis of oxygen vacancies (for details see [6–9] and references therein).

As regards the YAP:C and YAM:C samples, their emission intensity was much lower than for YAG:C and was hardly to register in our measuring conditions. The PLE spectra when registered at 385 nm (the most intensive PL line of Tb^{3+}) for YAP:C and YAM:C ceramic samples are shown in Fig. 4. These excitation spectra, beside the 273 nm band related to Tb^{3+} ions, consist of the broad band at 250 nm (major for YAM:C) and bands at 290 and 305 nm (major ones for YAP:C).

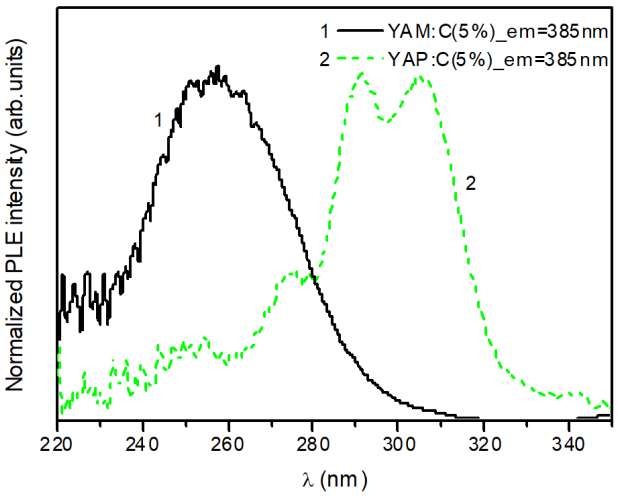

Fig. 4. Room temperature PLE spectra of YAP:C and YAM:C ceramic samples.

Temperature quenching of the emission related to F-type centers at elevated temperatures obtained for the YAG:C(5%) ceramics is shown in Fig. 5. As it is seen from the figure, the emission intensity undergoes quenching already at temperatures higher than 80 °C and disappears almost completely at temperatures about 400 °C. This observation is consistent with the quenching of F centers known in Al_2O_3:C [3, 10]. Typical thermal glow curves of the studied ceramic samples after ionizing irradiation are presented in Fig. 6. It is surprising that the TL intensity of the oxygen-deficient materials was usually lower than the intensity of the corresponding materials prepared in air. At the same time the structure of the thermal glow is similar for YAG, YAP, and YAM samples. Namely, the peaks at 150 and 200 °C are observed as the main ones. The observed peak structure is consistent with the results reported before for nominally pure and doped YAP and YAG (see e.g. [5, 11–14]) and is related most likely to Y_{Al} antisites in the studied materials. In such a way, after such kind of irradiation, we did not observe a thermal glow that could be related to oxygen vacancies in the oxygen-deficient materials.

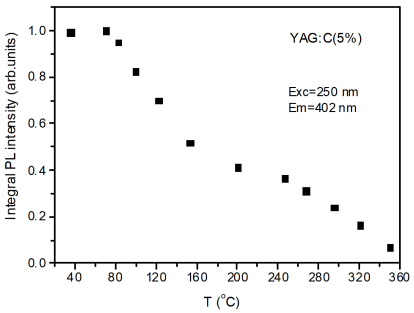

Fig. 5. Integral PL intensity of the YAG:C(5%) ceramics as a function of temperature.

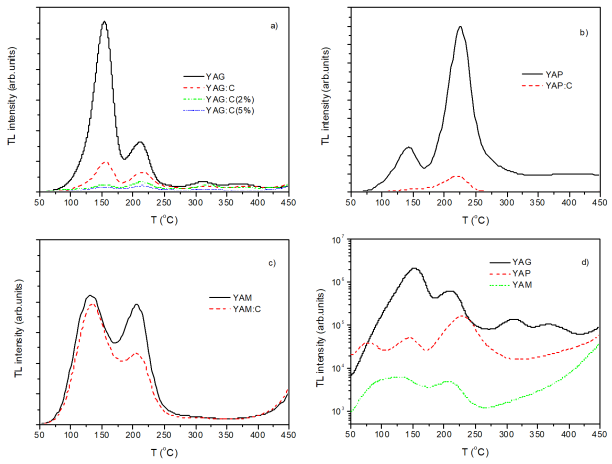

Fig. 6. Typical thermal glow curves of the studied ceramic samples registered just after β-irradiation at room temperature. Heating rate 4 °C/s.

Quite another situation is observed after UV exposure (we used the 254 or 302 nm lines of mercury lamp) that fits to the excitation bands related to F-type centers. After such kind of irradiation, the TL intensity of the oxygen-deficient samples is much higher with respect to the samples prepared in air (see Fig. 7). The thermal

glow structure at the same time is somewhat different from that after ionizing irradiation. Namely the broad TL peaks at 150–200 and 300 °C dominate. We are inclined to relate this thermal glow that increases in intensity with increase of the oxygen-deficiency, with oxygen vacancies in the materials.

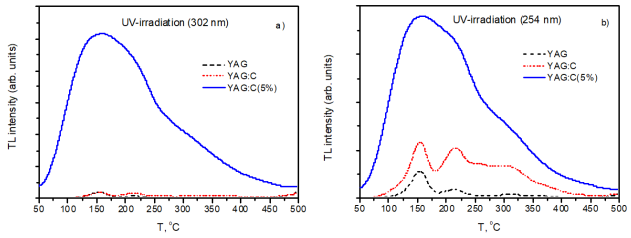

Fig. 7. Thermal glow curves of YAG and YAG:C ceramic samples registered just after UV light exposure at room temperature. Heating rate 4 °C/s.

4. Conclusions

Photoluminescence and thermoluminescence studies of the oxygen-deficient YAG, YAP, and YAM phosphors were performed. The studies reveal that the luminescent properties of the materials are related not only to the *F*-type centers created on the basis of oxygen vacancies, but also to other point defects, such as antisites (Y_{Al}) and uncontrolled impurity ions like Tb^{3+}. This complicates situation in comparison with the oxygen-deficient Al_2O_3.

Thermoluminescent properties of the studied materials after ionizing irradiation were revealed to be caused mainly by the Y_{Al} anisites, whereas *F*-type centers became visible in thermoluminescence after UV light exposure.

Acknowledgments

The work was supported by the NATO Science for Peace and Security Program (Project G4649), by the Ministry of Education and Science of Ukraine (project DB/Reader), and by the European Regional Development Fund (Innovative Economy grant POIG.01.01.02-00-108/09).

References

[1] M.S. Kulkarni, K.P. Muthe, N.S. Rawat, D.R. Mishra, M.B. Kakade, S. Ramanathan, S.K. Gupta, B.C. Bhatt, J.V. Yakhmi, D.N. Skarm, *Radiat. Meas.* **43**, 492 (2008).

[2] M.S. Akselrod, V.S. Kortov, D.J. Kravetsky, V.I. Gotlib, *Radiat. Prot. Dosim.* **32**, 15 (1990).

[3] S.V. Kortov, I.I. Milman, V.I. Kirpa, J. Lesz, *Radiat. Prot. Dosim.* **55**, 279 (1994).

[4] S.W.S. McKeever, M.W. Blair, E. Bulur, R. Gaza, R. Gaza, R. Kalchgruber, D.M. Klein, E.G. Yukihara, *Radiat. Prot. Dosim.* **109**, 269 (2004).

[5] Ya. Zhydachevskii, I. Kamińska, K. Fronc, A. Reszka, W. Paszkowicz, S. Warchol, M. Berkowski, D. Elbaum, A. Suchocki, *Opt. Mater.* **37**, 125 (2014).

[6] Y. Zorenko, T. Zorenko, T. Voznyak, A. Mandowski, Qi Xia, M. Batentschuk, J. Friedrich, *IOP Conf. Series Mater. Sci. Eng.* **15**, 012060 (2010).

[7] L. Grigorjeva, D. Jankoviča, K. Smits, D. Millers, S. Zazubovich, *Latv. J. Phys. Techn. Sci.* **4**, 54 (2012).

[8] A. Matkovski, D. Sugak, S. Melnyk, A. Suchocki, Z. Frukacz, *J. Alloys Comp.* **300-301**, 395 (2000).

[9] S.B. Ubizskii, A.O. Matkovski, N.A. Mironova-Ulmane, V. Skvortsova, A. Suchocki, Y.A. Zhydachevskii, P. Potera, *Nucl. Instrum. Methods Phys. Res. B* **166-167**, 40 (2000).

[10] M.S. Akselrod, N. Agersnap Larsen, V. Whitley, S.W.S. McKeever, *J. Appl. Phys.* **84**, 3364 (1998).

[11] Ya. Zhydachevskii, A. Durygin, A. Suchocki, A. Matkovskii, D. Sugak, Z. Frukacz, *Phys. Status Solidi C* **1**, 312 (2004).

[12] Ya. Zhydachevskii, A. Suchocki, M. Berkowski, D. Sugak, A. Luchechko, S. Warchol, *J. Cryst. Growth* **310**, 3219 (2008).

[13] M. Baran, Ya. Zhydachevskii, A. Suchocki, A. Reszka, S. Warchol, R. Diduszko, A. Pajączkowska, *Opt. Mater.* **34**, 604 (2012).

[14] Ya. Zhydachevskii, I.I. Syvorotka, L. Vasylechko, D. Sugak, I.D. Borshchyshyn, A.P. Luchechko, Ya.I. Vakhula, S.B. Ubizskii, M.M. Vakiv, A. Suchocki, *Opt. Mater.* **34**, 1984 (2012).